An Analysis of Stability Margins for Continuous Systems

Julie C. Albanus

Thesis submitted to the Faculty of the
Virginia Polytechnic Institute and State University
in partial fulfillment of the requirements for the degree of

Master of Science in Mathematics

Terry L. Herdman, Chairman
John A. Burns
Jeff Borggaard

May 1999

Falls Church, Virginia

Keywords: Controllability Radius, Stabilizability Radius, Stability Margin

An Analysis of Stability Margins for Continuous Systems

Julie C. Albanus

(ABSTRACT)

When designing or reviewing control systems, it is important to understand the limitations of the system's design. Many systems today are designed using numerical methods. Although the numerical model may be controllable, stabilizable, or stable, small perturbations of the system parameters can result in the loss of these properties. In this thesis, we investigate these issues for finite element approximations of a thermal convection loop.

Acknowledgments

I would like to thank Dr. Terry L. Herdman for his continuing guidance, faith, encouragement, and support, and most of all for bringing the opportunity to further study mathematics at Virginia Tech to Northern Virginia.

I would also like to thank Dr. John A. Burns for introducing me to this interesting area of mathematics and for challenging me to take on this problem. You were right when you said that delving into this project could take years.

An Analysis of Stability Margins for Continuous Systems

Table of Contents:

Figures and Tables:

Chapter 1: Introduction

As computational systems become more capable and less expensive, numerical approximation of mathematical systems has become a very dynamic field. The systems grow in complexity, and the measurements become more refined. An important factor in the development of any system using numerical approximation is the margin of error for the approximation.

The discussion herein looks at the margin of error for a continuous control system defined for a thermal convection loop. Chapter 2 discusses the measurements that will be used to analyze the system—controllability, stabilizability, and stability radii. Chapter 3 discusses thermal convection loop, the partial differential equation (PDE) model, and the finite element approximation. The goal is to control the flow of the fluid in the thermal convection loop by means of controlling the temperature of the walls. The application model and approximation are taken from a paper by Burns, King, and Rubio [4] and Dr. Rubio's dissertation [18].

The intent of this paper is to determine how changes in the key parameters associated with the thermal convection loop affect the controllability, stabilizability, and stability of the system. The key parameters that will be investigated are kinematic viscosity ν, the thermal expansion β, and thermal diffusivity χ. These parameters are identified as the PDE model is discussed in Chapter 2. All three are properties of the viscous fluid used in the thermal convection loop. The thermal expansion coefficient provides the coupling between the velocity and thermal fields and hence plays an important role in system stabilizability and controllability. Although control effectiveness changes as the thermal expansion coefficient increases, it is not clear how system stabilizability and

controllability radii are impacted. This is the primary focus of the study.

Three cases will be considered for each set of parameter values. These cases are determined by the control applied to the system. The control may be applied to the inner wall, to the outer wall, or to both walls. In normal circumstances applying the control to the outer wall should have larger controllability and stabilizability radii than applying the control only to the inner wall. This is because of the larger surface area on the outer wall. Similarly, applying the control to both walls should provide greater controllability and stabilizability radii than either of the other two cases for similar reasons. However, since the problem considered here is defined by a thin loop, it is not clear that these differences are significant.

Chapter 2: Control System Radii

2.1 Control System Definition

$$(\Sigma_n) \quad \begin{aligned} \dot{\mathbf{x}}(t) &= \mathbf{A}\mathbf{x}(t) + \mathbf{B}\mathbf{u}(t) \\ \mathbf{y}(t) &= \mathbf{C}\mathbf{x}(t) \end{aligned} \tag{2.1.1}$$

Let $\Sigma_n = (\mathbf{A}, \mathbf{B}, \mathbf{C})$ denote the linear, time invariant, finite dimensional system of dimension n, where **A**, **B**, and **C** are $n \times n$, $n \times m$ and $l \times n$ real matrices, respectively. In Σ_n above, $\mathbf{x}(t)$ is the state vector, $\mathbf{u}(t)$ is the control, and $\mathbf{y}(t)$ is the output. For a given initial condition $\mathbf{x}(0)=\mathbf{x}_0$, a control $\mathbf{u}(t)$, and $L_2(0,t)$, there is a solution to (2.1.1) given by the variation of parameter formula (see [16]).

$$\mathbf{x}(t) = e^{\mathbf{A}t}\mathbf{x}_0 + \int_0^t e^{\mathbf{A}(t-s)}\mathbf{B}\mathbf{u}(s)ds \tag{2.1.2}$$

2.2 Controllability and Stabilizability

Information can be gained about a control system by evaluating several properties of the system. These properties include controllability, observability, stabilizability, and detectability. Observability and detectability are further discussed in [15] and will not be discussed here. The focus of this paper is on the properties of controllability and stabilizability, which are defined as follows.

Definition 2.2.1. The system Σ_n is controllable if given $\mathbf{x}_0$, $\mathbf{x}_1 \in \mathbb{R}^n$ and $t_1 > 0$, there is a control $\mathbf{u}(\cdot)$ in $L_2(0,t_1)$ such that $\mathbf{x}(0)=\mathbf{x}_0$ and $\mathbf{x}(t_1)=\mathbf{x}_1$ where $\mathbf{x}(t)$ is defined by (2.1.2).

Definition 2.2.2. The system Σ_n is exponentially stabilizable if there is an $m \times n$ matrix **K** and positive

numbers M and α such that if $\mathbf{u}(t) = -\mathbf{K}\mathbf{x}(t)$ then the closed loop system $\dot{\mathbf{x}}_c(t) = [\mathbf{A} - \mathbf{B}\mathbf{K}]\mathbf{x}_c(t)$ has solutions $\mathbf{x}_c(t)$ satisfying $\|\mathbf{x}_c(t)\| \leq Me^{-\alpha t}\|\mathbf{x}_c(0)\|$ for all $t \geq 0$.

There are several equivalent matrix norms. In Definition 2.2.2, we consider the specific case where we use the spectral norm. A definition of the spectral norm may be found in [15].

It is valuable to relate the property definitions above to the control system matrices (i.e. **A**, **B**, and **C**). The following theorem helps establish a relationship between the controllability and the system matrices. The proof may be found in [11, 17].

Theorem 2.2.1. The linear system Σ_n is controllable if and only if the controllability matrix, $\mathbf{CM} = [\mathbf{B}, \mathbf{AB}, \mathbf{A}^2\mathbf{B}, ..., \mathbf{A}^{n-1}\mathbf{B}]$, has rank n.

Considering $\mathbf{H}(\lambda) = [\lambda\mathbf{I}\text{-}\mathbf{A}, \mathbf{B}]$, the following theorems may be found in [15] and [2].

Theorem 2.2.2. The linear system Σ_n is controllable if and only if rank $\mathbf{H}(\lambda) = n$ for all $\lambda \in C$.

Theorem 2.2.3. The linear system Σ_n is stabilizable if and only if rank $\mathbf{H}(\lambda) = n$ for all $\lambda \in C$ with $\mathrm{Re}(\lambda) \geq 0$.

When analyzing a control system, it should be realized that if a system is controllable (or stabilizable), then there is a neighborhood of controllable (or stabilizable) systems around the given system. In other words, the system will remain controllable (or stabilizable) for sufficiently small

perturbations of the system matrices. This leads to the discussion of what is "sufficiently small" and the definition of control system radii.

2.3 Controllability and Stabilizability Radii

Many researchers and designers recognize the significance of determining the control system radii when analyzing algorithms of control design. Discussions of this can be found in [1,6,8,12,13,14]. Put simply, if the distance between the control system and any uncontrollable system is small, then small errors in defining the system matrices may destroy controllability. Additionally, if an algorithm makes assumptions of controllability (or stabilizability), then the algorithm will likely be numerically ill conditioned, or unreliable, for systems nearly uncontrollable (or nearly unstabilizable). The relationship between the control problem condition number and the distance to the nearest ill-posed problem are discussed by Laub [12,14] and by Demmel [6, 7].

Control system radii can be evaluated in terms of both real and complex sets. The control system analysis that follows will use the complex radii of controllability and stabilizability, so that is the primary focus here. Consider the following sets of systems;

$$\Gamma = \{\Sigma = (\mathbf{A}, \mathbf{B}, \mathbf{C}) \,|\, \mathbf{A} \in \mathrm{C}^{nxn}, \mathbf{B} \in \mathrm{C}^{nxm}, \mathbf{C} \in \mathrm{C}^{lxn}\},$$

$$\Omega = \{\Sigma = (\mathbf{A}, \mathbf{B}, \mathbf{C}) \in \Gamma \,|\, \mathbf{A} \in \mathrm{R}^{nxn}, \mathbf{B} \in \mathrm{R}^{nxm}, \mathbf{C} \in \mathrm{R}^{lxn}\}.$$

Note that Ω is a subset of Γ. The distance between two elements of Γ, $\Sigma^1=(\mathbf{A}_1,\mathbf{B}_1,\mathbf{C}_1)$ and $\Sigma^2=(\mathbf{A}_2,\mathbf{B}_2,\mathbf{C}_2)$, is defined by $\delta(\Sigma^1,\Sigma^2) = \|(\mathbf{A}_1 - \mathbf{A}_2, \mathbf{B}_1 - \mathbf{B}_2, \mathbf{C}_1 - \mathbf{C}_2)\|_2$, where $\|\ \|_2$ is the Frobenius norm.

Further, if S is a subset of Γ and Σ is an element of Γ, then the distance between Σ and S is defined by $\mathrm{d}(\Sigma, S) = \inf\{\delta(\Sigma, \Sigma^j) \,\big|\, \Sigma^j \in S\}$.

Let $N_c \subseteq \Gamma$ be the set of all complex systems that are not controllable, and $N_s \subseteq \Gamma$ be the set of all complex systems that are not stabilizable. Given $\Sigma \in \Gamma$, the complex controllability radius, γ_c, and complex stabilizability radius, γ_s, are defined by

$$\gamma_c = \gamma_c(\Sigma) = \mathrm{d}(\Sigma, N_c),$$

and

$$\gamma_s = \gamma_s(\Sigma) = \mathrm{d}(\Sigma, N_s),$$

respectively.

The above definitions do not easily provide the actual value of the controllability or stabilizability radius for a given system. To compute these control system radii for a given system, the following theorems from [8] are helpful.

As a foundation for the theorems, it is important to understand the minimum singular value of a matrix. The minimum singular value of a matrix **M**, denoted by $\sigma_{\min}(\mathbf{M})$, indicates the distance to the nearest rank deficient matrix (see [9]). Since Theorems 2.2.1 and 2.2.2 both state that a given system is controllable if and only if the matrix being used (i.e. **CM** or $\mathbf{H}(\lambda)$) has full rank, it is clear that the minimum singular value will be useful in determining the distance to the nearest uncontrollable system. The following results may be found in [3] and [8].

Theorem 2.3.1. If Σ is controllable, then

$$\gamma_c = \gamma_c(\Sigma) = \min_{\lambda \in \mathbf{C}} \{\sigma_{\min}[\mathbf{H}(\lambda)]\}.$$

Theorem 2.3.2. If Σ is stabilizable, then

$$\gamma_s = \gamma_s(\Sigma) = \min_{\mathrm{Re}(\lambda) \geq 0} \{\sigma_{\min}[\mathbf{H}(\lambda)]\}.$$

As mentioned before, these values can also be determined using only real perturbations of the system matrices. The real controllability radius, ω_c, and stabilizability radius, ω_s, are defined as

$$\omega_c = \omega_c(\Sigma) = \mathrm{d}(\Sigma, N_c \cap \Omega), \quad \text{and}$$

$$\omega_s = \omega_s(\Sigma) = \mathrm{d}(\Sigma, N_s \cap \Omega).$$

Computing these real control radii is not without complication. This paper centers on the complex radii, and for this reason will not discuss further the real radii, other than to mention that the complications and common errors in calculating the real control system radii are discussed more fully in [15].

Since controllability implies stabilizability, it follows that $\gamma_c \leq \gamma_s$. That is, the distance from a given system to the nearest uncontrollable system has to be less than or equal to the distance to the nearest unstabilizable system.

Other interesting results can be found in the paper by Burns and Peichl [3]. These results apply to specific types of matrices.

Theorem 2.3.3. Assume that $\Sigma = (\mathbf{A},\mathbf{B},\mathbf{C}) \in \Gamma$ is controllable.

(i) If $\mathbf{A} = \mathbf{A}^*$, then

$$\gamma_c = \min_{\lambda \in \mathbb{R}} \{\sigma_{\min}[\mathbf{H}(\lambda)]\}.$$

(ii) If $\mathbf{A} = -\mathbf{A}^*$, then

$$\gamma_c = \min_{\lambda \in \mathbb{R}} \{\sigma_{\min}[\mathbf{H}(i\lambda)]\}.$$

(iii) If $\Sigma = (\mathbf{A},\mathbf{B},\mathbf{C}) \in \Omega$ and $\mathbf{A} = \mathbf{A}^T$, then

$$\gamma_c = \omega_c = \min_{\lambda \in \mathbb{R}} \{\sigma_{\min}[\mathbf{H}(\lambda)]\}.$$

Theorem 2.3.4. Assume that $\Sigma = (\mathbf{A},\mathbf{B},\mathbf{C}) \in \Gamma$ is stabilizable and let $R^+ = \{\lambda \in R \mid \lambda > 0\}$.

(iv) If $\mathbf{A} = \mathbf{A}^*$, then

$$\gamma_s = \min_{\lambda \in R^+} \{\sigma_{\min}[\mathbf{H}(\lambda)]\}.$$

(v) If $\mathbf{A} = -\mathbf{A}^*$, then

$$\gamma_s = \min_{\lambda \in R} \{\sigma_{\min}[\mathbf{H}(i\lambda)]\}.$$

(vi) If $\Sigma = (\mathbf{A},\mathbf{B},\mathbf{C}) \in \Omega$ and $\mathbf{A} = \mathbf{A}^T$, then

$$\gamma_s = \omega_s = \min_{\lambda \in R^+} \{\sigma_{\min}[\mathbf{H}(\lambda)]\}.$$

Corollary 2.3.1. If $\Sigma = (\mathbf{A},\mathbf{B},\mathbf{C}) \in \Omega$ is stabilizable, $\mathbf{A} = \mathbf{A}^T$, and $\mathbf{x}^T\mathbf{A}\mathbf{x} \leq 0$ for all $\mathbf{x} \in R^n$, then

$$\gamma_s = \omega_s = \sigma_{\min}[\mathbf{H}(0)] = \sigma_{\min}[\mathbf{A},\mathbf{B}].$$

Corollary 2.3.1 has applications to a variety of finite element and finite difference approximations of the heat equation. The application chosen for study of the control system properties discussed in this chapter is a thermal convection loop, which involves the heat equation. A finite element approximation will be used. The application and associated approximations are discussed in the next chapter.

Chapter 3: The Thermal Convection Loop

3.1 Physical Description

The application chosen for analysis is a thermal convection loop. Convection is conduction heat transfer accelerated by the motion of the fluid. Figure 3.1 illustrates the loop. A circular pipe contains a viscous fluid. The pipe is standing in the vertical plane. The forces acting on the fluid include the force due to gravitational acceleration and the buoyancy force.

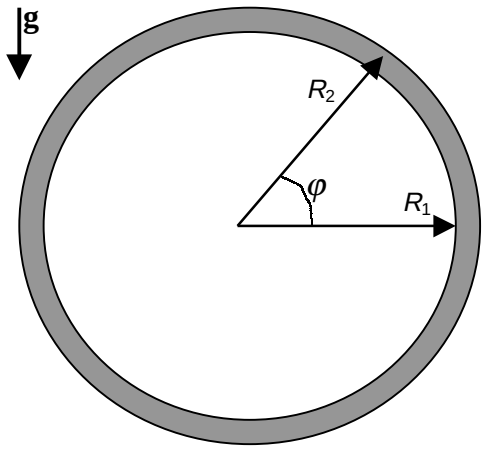

FIGURE 3.1
Description of a thermal convection loop

If there is a temperature gradient, with cooler fluid at the top and warmer fluid below, the buoyancy force tends to generate fluid motion. Viscosity and thermal diffusivity resist the motion. The position of a fluid particle is given by radial, r, and angular, φ, coordinates where $r \in [R_1, R_2]$.

For a more detailed discussion of the thermal convection loop see [4,18].

3.2 The PDE Model

This section briefly discusses the basic assumptions and approximations used to develop the partial differential equation model of this system. Three key parameters are identified that will be used later in the numerical experiments to analyze the control system. These parameters are kinematic viscosity ν,

gravitational acceleration times thermal expansion $g\beta$, and thermal diffusivity χ.

Assuming a thin pipe, where pipe width is small compared to the interior radius (i.e. R_2-R_1<<R_1), allows the approximation of fluid flowing in a straight pipe. That is, the velocity depends only on the radial position r. Additionally, it is assumed that the fluid flow has circular streamlines, meaning that the fluid particles remain a fixed distance from the pipe walls. Based on these assumptions, the velocity vector **v** can be represented as

$$\mathbf{v}(t,r,\varphi) = v(t,r)\mathbf{e}_{\varphi}.$$

The equations of motion for a Newtonian viscous flow are used. The equations are given by

$$\frac{\partial \mathbf{v}}{\partial t} + (\mathbf{v}\cdot\nabla)\mathbf{v} = \frac{1}{\rho}\mathbf{F}_g - \frac{1}{\rho}\nabla p + \upsilon\Delta\mathbf{v} + \left(\frac{\mu+\lambda}{\rho}\right)\nabla(\text{div }\mathbf{v})\,\frac{\partial\rho}{\partial t} + \text{div}(\rho\mathbf{v}) = 0$$

where ρ is density, $\mathbf{F}_g$ is the body force per unit mass, μ and λ are coefficients of viscosity, and p is the pressure. Kinematic viscosity, ν, is the absolute viscosity, μ, divided by density, or $\nu = \mu / \rho$. The relationship between the density and the temperature, T, is assumed to be linear, where

$$\rho = \overline{\rho}_0(1 - \beta(T - \overline{T}_0)) \qquad (3.2.1)$$

The terms $\overline{\rho}_0$ and $\overline{T}_0$ are the reference density and temperature for the system, generally a system average. For this model, $T(t,r,\varphi)$ is considered to be the variation from a room temperature value, or the reference temperature. Note that the thermal expansion coefficient, β, quantifies the change in density for a given change in temperature. The external force per unit mass $\mathbf{F}_g$ is based upon gravitational acceleration and the buoyancy force. The equation for $\mathbf{F}_g$ is given by

$$\mathbf{F}_g = \rho\mathbf{g} + \overline{\rho}_0\mathbf{g}\beta(\overline{T}_0 - T)$$

To complete the system description, heat transfer must be included using the heat equation,

$$\frac{\partial T}{\partial t} + \mathbf{v} \cdot \nabla T = \chi \Delta T$$

Note that χ is the coefficient of thermal diffusivity.

The Boussinesq approximations are used, assuming all system parameters are constant except for density in the buoyancy term. This approximation is valid for small changes in density. The implication is that div **v** = 0 as in the incompressible Navier-Stokes equations. Combining the incompressible Navier-Stokes and the heat equation provides the Boussinesq equations:

$$\frac{\partial \mathbf{v}}{\partial t} + (\mathbf{v} \cdot \nabla)\mathbf{v} = \mathbf{g}(1 + \beta(\overline{T_0} - T)) - \frac{1}{\rho}\nabla p + \upsilon \Delta \mathbf{v}$$

$$\text{div } \mathbf{v} = 0$$

$$\frac{\partial T}{\partial t} + \mathbf{v} \cdot \nabla T = \chi \Delta T$$

Using the assumptions and approximations above and denoting the magnitude of gravitational acceleration by g, the controlled system for $v(t,r)$, $T(t,r,\varphi)$ is governed by the nonlinear integro-partial differential equations.

$$\frac{\partial v}{\partial t}(t,r) = \frac{g\beta}{2\pi}\int_0^{2\pi} T(t,r,\varphi)\cos\varphi\, d\varphi + \upsilon \Delta_r v(t,r) \qquad (3.2.2)$$

$$\frac{\partial T}{\partial t}(t,r,\varphi) = -\frac{v(t,r)}{r}\frac{\partial T}{\partial \varphi}(t,r,\varphi) + \chi \Delta T(t,r,\varphi) \qquad (3.2.3)$$

Initial conditions $v_0(r)$ and $T_0(r, \varphi)$ are given by

$$v(0,r) = v_0(r), \quad R_1 < r < R_2$$

$$T(0,r,\varphi) = T_0(r,\varphi), \quad R_1 < r < R_2, \quad 0 \le \varphi < 2\eth$$

Boundary conditions for the velocity are given by $\mathbf{v}(t,R_1) = \mathbf{v}(t,R_2) = 0$. In the numerical experiments that follow three cases will be investigated for each set of parameters– (1) only

the inner wall is controlled, (2) only the outer wall is controlled, and (3) both walls are controlled. On the uncontrolled boundary, $T(t, r, \varphi) = 0$ when $t > 0$ and $\varphi \in [0,2\pi)$. On the controlled boundary, $T(t, r, \varphi) = u(t,\varphi)$ when $t < 0$ and $\varphi \in [0,2\pi)$, where $u(t,\varphi)$ is the Dirichlet boundary control.

3.3 Finite Element Approximation of the System

A Galerkin-based finite element approximation scheme is applied to the variational form of the Boussinesq model of the problem. In an abstract formulation, this problem has the form

$$< \dot{\mathbf{z}}(t), \omega > = < (-\mathbf{A}_0)^{1/2}\mathbf{z}(t), (-\mathbf{A}_0)^{1/2}\omega > + < \mathbf{A}_1\mathbf{z}(t), \omega >$$
$$+ < f(\mathbf{z}(t)), \omega > + < \mathbf{G}\eta(t), \omega > + < \mathbf{u}(t), \mathbf{B}^*\omega >,$$

where $-\mathbf{A}_0$ is the linear part of the dynamic operators (see [18] for details). Uniform triangulation of the polar plane creates the sector elements. The approximate velocity is obtained using Lagrangian quadratic elements in R with basis $\{\Phi_k^h, 1 \le k \le N_v\}$. For temperature, piecewise bilinear functions are used with basis $\{\Psi_k^h, 1 \le k \le N_T\}$. The basis for the full product space is

$$B = \left\{ \begin{pmatrix} \Phi_1^h \\ 0 \end{pmatrix}, \begin{pmatrix} \Phi_2^h \\ 0 \end{pmatrix}, \cdots, \begin{pmatrix} \Phi_{N_v}^h \\ 0 \end{pmatrix}, \begin{pmatrix} 0 \\ \Psi_1^h \end{pmatrix}, \begin{pmatrix} 0 \\ \Psi_2^h \end{pmatrix}, \cdots, \begin{pmatrix} 0 \\ \Psi_{N_T}^h \end{pmatrix} \right\}$$

A full discussion of the development of the finite element approximation may be found in [18], but the construction of the system matrices is of interest here. Below are representations of the matrices $\mathbf{A}^h$ and $\mathbf{B}^h$. These may be useful in analyzing the controllability and stabilizability radii. The other system matrices can be found in [4].

$$\mathbf{A}^h = \begin{bmatrix} \mathbf{A}_v^h & \mathbf{A}_{l_v}^h \\ 0 & \mathbf{A}_T^h \end{bmatrix}, \text{ where}$$

$$\mathbf{A}_v^h = \left[\left\langle \Phi_i^h, \Phi_j^h \right\rangle_{L^2(\Omega_1)} \right]_{i,j=1\ldots N_v}^{-1} \left[-\nu \left\langle \left(\Phi_i^h\right)', \left(\Phi_j^h\right)' \right\rangle_{L^2(\Omega_1)} \right]_{i,j=1\ldots N_v}$$

$$\mathbf{A}_T^h = \left[\left\langle \Psi_i^h, \Psi_j^h \right\rangle_{L^2(\Omega)} \right]_{i,j=1\ldots N_T}^{-1} \left[-\chi \left\langle \left(\nabla\Psi_i^h\right), \left(\nabla\Psi_j^h\right) \right\rangle_{L^2(\Omega)} \right]_{i,j=1\ldots N_T}$$

$$\mathbf{A}_v^h = \left[\left\langle \Phi_i^h, \Phi_j^h \right\rangle_{L^2(\Omega_1)} \right]_{i,j=1\ldots N_v}^{-1} \left[\frac{g\beta}{2\pi} \left\langle \Phi_i^h, \int_0^{2\pi} \cos\varphi \Psi_j^h(\cdot,\varphi) d\varphi \right\rangle_{L^2(\Omega_1)} \right]_{i=1\ldots N_v, 1\le j\le N_T}$$

and,

$$\mathbf{B}^h = \begin{bmatrix} \mathbf{B}_v^h \\ \mathbf{B}_T^h \end{bmatrix}, \text{ where}$$

$$\mathbf{B}_v^h = \left[\left\langle \Phi_i^h, \Phi_j^h \right\rangle_{L^2(\Omega_1)} \right]_{i,j=1\ldots N_v}^{-1} \left[-\frac{g\beta R_2}{4\pi} \left\langle \cos\varphi \int_{R_1}^{R_2} \Phi_i^h(r) dr, l_j^h \right\rangle_{L^2(\Gamma_2)} \right]_{1\le i\le N_v, 1\le j\le N_T}$$

$$\mathbf{B}_T^h = \left[\left\langle \Psi_i^h, \Psi_j^h \right\rangle_{L^2(\Omega)} \right]_{i,j=1\ldots N_T}^{-1} \left[-\chi R_2 \left\langle \frac{\partial \Psi_i^h}{\partial \eta}, l_j^h \right\rangle_{L^2(\Gamma_2)} \right]_{1\le i\le N_v, 1\le j\le N_T}$$

Chapter 4: Numerical Results

4.1 Methodology

The numerical experiments conducted investigate trends in the calculated controllability and stabilizability radii for the system, [**A B**]. In addition, we solve an LQR problem for the optimal feedback gain K and analyze the stability radius for the closed loop system [**A**-**BK**]. Three cases are investigated for each set of parameter values. These cases depend on the applied control. In Case 1, the control is applied only to the inner wall, in Case 2, the control is applied only to the outer wall, and in Case 3, the control is applied to both walls.

All numerical computations are implemented in MATLAB. The system matrices, **A** and **B,** are constructed using the finite element approximation program developed by D. Rubio. The program builds matrices **A** and **B** and generates the feedback gain **K** based on the parameter values. The data that follows is consistently based on a finite element structure geometry of 5 radial and 10 angular segments. Additional runs of Case 1 were made using 8 radial and 32 angular segments. These runs confirmed the trends shown by the other segment divisions.

As discussed previously, the goal was to investigate how changes in system parameters affect the system properties. It was expected that, in general, the radii and margins would be less for Case 1 than for Case 2, and less for Case 2 than Case 3. These results are expected because of the amount of surface area being controlled. Case 1 (inner wall only) affects the least area, and Case 3 (both walls) affects the most.

In the numerical experiments, the accuracy of the controllability radius depends greatly on the search conducted. The results are a guaranteed upper bound for the controllability

radius, but must be viewed as estimates. Accuracy of the estimate varies with the control case and parameter values. Most of the values of the stabilizability radius are more accurate than the values for the controllability radius. This is because controllability radius values were generally found at negative real perturbations of the system matrices. That is, the minimum singular value of $\mathbf{H}(\lambda) = [\lambda\mathbf{I}-\mathbf{A}, \mathbf{B}]$ came from $\lambda = \mathrm{Re}(\lambda)$ and $\lambda < 0$. Thus, the minimum singular value of $\mathbf{H}(\lambda)$ for the stabilizability radius was typically found at $\lambda = 0$.

Also, of interest was how changes in the system parameters-- kinematic viscosity ν, gravitational acceleration and thermal expansion $g\beta$, and thermal diffusivity χ -- would affect the controllability or stabilizability of the system. Each of these parameters was varied independently of the others. The detailed results of these analyses follow. Graphs are shown for the stabilizability radius and stability margin to help demonstrate the trends exhibited by the data.

4.2 Variations in the Thermal Expansion Coefficient

A broad range of values for $g\beta$ was considered. It was initially expected that as $g\beta$ increased, would also increase the system margin to controllability and stabilizability. This was expected because of the prominence of $g\beta$ in equation (3.2.2). However, this turned out not to be the case.

The data in Table 4.2 shows how the stabilizability radius, γ_s, of the open loop system [**A B**], and the stability margin of the closed loop system, $s_r = \min_{\lambda \in R} \sigma_{\min}(\lambda I - A)$, decrease as $g\beta$ increases. As discussed above, the controllability radius values are excluded here because they are smaller and less

reliable measurements of trend as compared to the other two properties. The stabilizability radius (Figure 4.2.1) and stability margin (Figure 4.2.2) data may also be seen in the graphical representations that follow.

TABLE 4.2 Variations in the Thermal Expansion Coefficient

RUN	$g\beta$ [ft/(s^{2}F)]	ν [ft^2/s]	χ[ft^2/s]	*CASE*	γ_c	γ_s	s_r
1	1.280e+01	1.627e-05	3.028e-06	*1*	0.00009	0.00013	0.00020
				2	0.00001	0.00018	0.00009
				3	0.00029	0.00032	0.00022
2	2.560e+00	1.627e-05	3.028e-06	*1*	0.00001	0.00017	0.00082
				2	0.00003	0.00081	0.00045
				3	0.00046	0.00122	0.00096
3	1.280e+00	1.627e-05	3.028e-06	*1*	0.00003	0.00021	0.00117
				2	0.00006	0.00149	0.00088
				3	0.00068	0.00169	0.00164
4	2.560e-01	1.627e-05	3.028e-06	*1*	0.00027	0.00070	0.00151
				2	0.00028	0.00226	0.00336
				3	0.00131	0.00227	0.00411
5	1.024e-01	1.627e-05	3.028e-06	*1*	0.00028	0.00153	0.00183
				2	0.00064	0.00271	0.00480
				3	0.00149	0.00271	0.00470
6	2.560e-03	1.627e-05	3.028e-06	*1*	0.00008	0.00320	0.00594
				2	0.00000	0.00400	0.00624
				3	0.00014	0.00401	0.01134
7	2.560e-04	1.627e-05	3.028e-06	*1*	0.00001	0.00320	0.00596
				2	0.00001	0.00400	0.00624
				3	0.00001	0.00401	0.01147
8	2.560e-05	1.627e-05	3.028e-06	*1*	0.00000	0.00320	0.00596
				2	0.00000	0.00400	0.00624
				3	0.00000	0.00401	0.01147

Since g is the constant for gravitational acceleration, changes in $g\beta$ may be discussed only in terms of β, the thermal expansion coefficient. Recalling equation (3.2.1) from the development of the PDE model for the system, it can be shown that, for a given temperature difference, as β increases the change in density decreases.

$$\rho = \overline{\rho}_0(1 - \beta \uparrow (T - \overline{T}_0)) \downarrow \quad \Rightarrow \quad \rho \downarrow$$

The change in density is what creates the buoyancy force, which in turn drives the motion of the fluid. Less motion for a given temperature difference means greater variation of temperatures are required to control the system; and thus, the controllability, the ability to get the system to the desired velocity in the desired time, is more difficult.

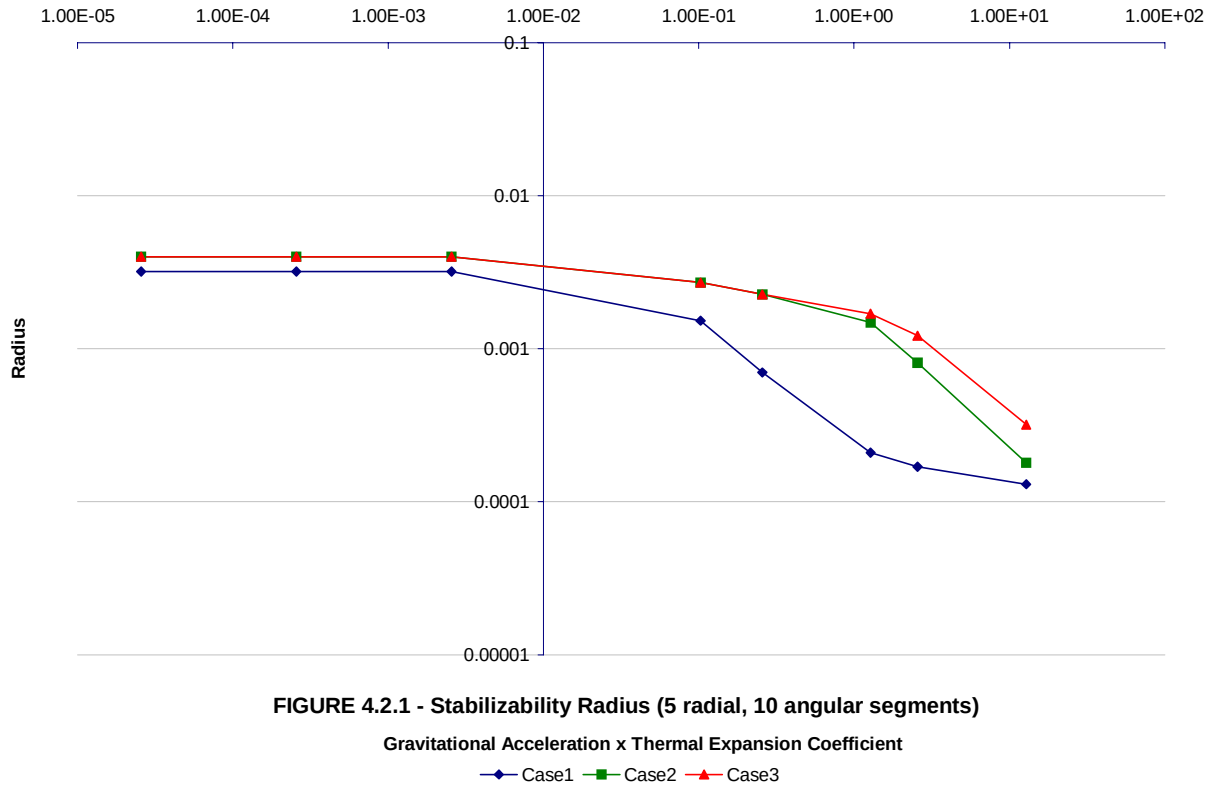

FIGURE 4.2.1 - Stabilizability Radius (5 radial, 10 angular segments)

For most of the runs, the data is consistent with the expectations for Case 1 properties to be less than Case 2 properties, and for Case 2 properties to be less than Case 3 properties. The runs representing the largest values of $g\beta$, Runs 1 through 3, do not meet this expectation. For these runs the range of open loop eigenvalues was noticeably different from the range of closed loop eigenvalues. Experiments have shown that

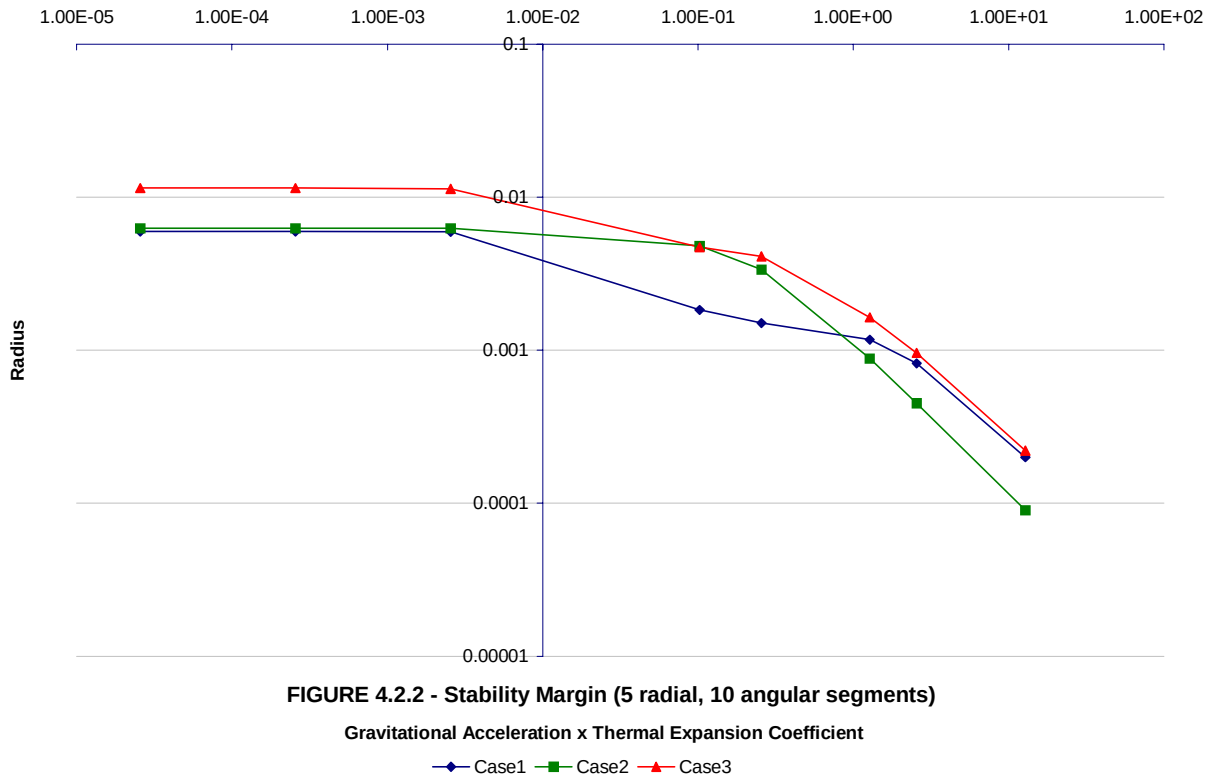

FIGURE 4.2.2 - Stability Margin (5 radial, 10 angular segments)

for large temperature differences, the fluid exhibits unstable motion (see [5,20,21]). The unexpected results of the runs involving the largest values of $g\beta$ may result from this unstable motion.

4.3 Variations in the Kinematic Viscosity Coefficient

The data for changes in the kinematic viscosity coefficient shows an inverse relationship for stabilizability and stability

than that of thermal expansion. As kinematic viscosity increases the stability and stabilizability increase as shown in Figures 4.3.1 and 4.3.2. This relationship is not unexpected. The kinematic viscosity of the fluid resists the fluid motion caused by the buoyancy force.

The values for stabilizability radii and stability margins, shown in Table 4.3, also vary as expected for the three control cases. Case 1 properties are less than Case 2 and 3 properties. It can be noted in the data that the stabilizability radius for Cases 2 and 3 are essentially equal for most of the runs. Although, in most cases, the stability margin for Case 2 is closer to the value for Case 1.

TABLE 4.3 Variations in the Kinematic Viscosity Coefficient

RUN	$g\beta$ [ft/(s^{2}F)]	ν [ft^2/s]	χ[ft^2/s]	*CASE*	γ_c	γ_s	s_r
1	2.560e-03	1.627e-03	3.028e-06	*1*	0.00007	0.00320	0.00596
				2	0.00007	0.00400	0.00624
				3	0.00010	0.00401	0.01147
2	2.560e-03	1.627e-04	3.028e-06	*1*	0.00007	0.00320	0.00596
				2	0.00018	0.00400	0.00624
				3	0.00011	0.00401	0.01147
3	2.560e-03	1.627e-05	3.028e-06	*1*	0.00008	0.00320	0.00594
				2	0.00000	0.00400	0.00624
				3	0.00014	0.00401	0.01134
4	2.560e-03	1.627e-06	3.028e-06	*1*	0.00008	0.00153	0.00156
				2	0.00001	0.00161	0.00166
				3	0.00000	0.00161	0.00175
5	2.560e-03	1.627e-07	3.028e-06	*1*	0.00004	0.00016	0.00033
				2	0.00003	0.00041	0.00049
				3	0.00012	0.00042	0.00056

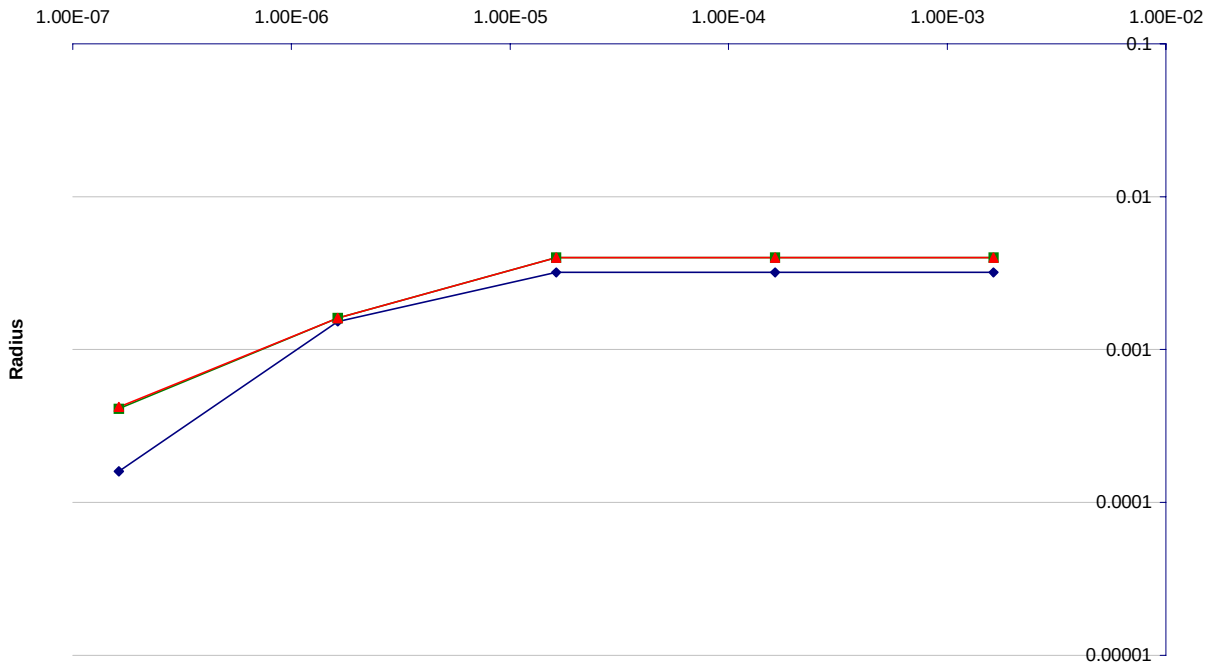

FIGURE 4.3.1 - Stabilizability Radius (5 radial, 10 angular segments)

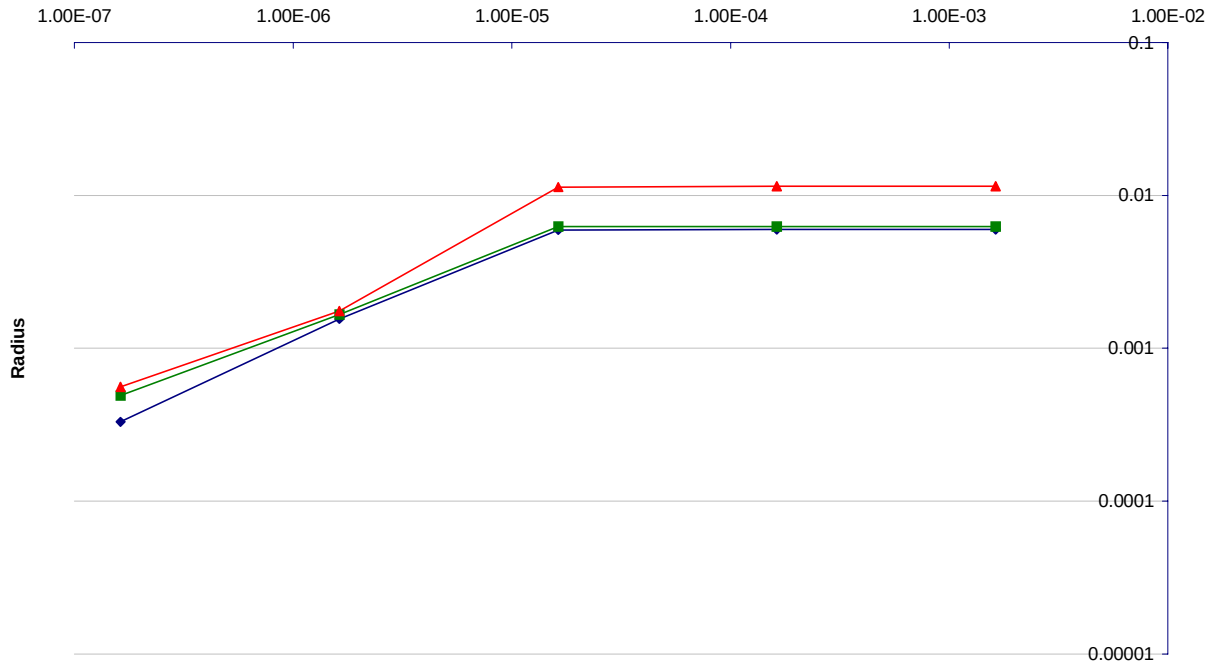

FIGURE 4.3.2 - Stability Margin (5 radial, 10 angular segments)

Both sets of graphs, for the kinematic viscosity coefficient and for the thermal expansion coefficient, exhibit asymptotic behavior as the stabilizability radius or stability margin approach the maximum values. This would indicate that a point exists after which changes in these parameters will have no further affect on the system properties. Smaller values of kinematic viscosity and larger values of thermal expansion can reduce the stability margin of the closed loop system and the stabilizability radius of the open loop system, but neither offers much possibility of increasing the system stability over that of water at room temperature.

4.4 Variations in the Thermal Diffusivity Coefficient

The thermal diffusivity coefficient exhibits a similar relationship to the system properties as that of the kinematic viscosity coefficient. However, of the three key parameters, thermal diffusivity seems to have the strongest ability to affect stabilizability and the closed loop stability margin. The values of the stabilizability radius, γ_s, and the stability margin, s_r, for any given parameter set are more consistent between cases than seen for the variations in the other two parameters. This can be seen in the values in Table 4.4 as well as in the graphs of stabilizability radius (Figure 4.4.1) and stability margin (Figure 4.4.2).

It was noted during the experiments that the relative minimum values of $\sigma_{\min}[\mathbf{H}(\lambda)]$ seem to occur at the same values of λ for all three, control cases of the given parameter set. The absolute minimum would be one of the relative minimums, but not necessarily the same one for all three cases. If further investigation of this application is conducted this phenomena

may lend some insight into the relationship between the control cases, system parameters, and system properties.

TABLE 4.4 Variations in the Thermal Diffusivity Coefficient

RUN	$g\beta$ [ft/(s^{2}F)]	ν [ft^2/s]	χ[ft^2/s]	*CASE*	γ_c	γ_s	s_r
1	2.560e-03	1.627e-05	3.028e-04	*1*	0.00010	0.01579	0.01580
				2	0.00003	0.01580	0.01580
				3	0.00013	0.01580	0.01581
2	2.560e-03	1.627e-05	3.028e-05	*1*	0.00009	0.01579	0.01579
				2	0.00000	0.01579	0.01580
				3	0.00015	0.01579	0.01581
3	2.560e-03	1.627e-05	3.028e-06	*1*	0.00138	0.00320	0.00594
				2	0.00235	0.00400	0.00624
				3	0.00237	0.00401	0.01134
4	2.560e-03	1.627e-05	3.028e-07	*1*	0.00003	0.00032	0.00059
				2	0.00014	0.00040	0.00062
				3	0.00019	0.00040	0.00114
5	2.560e-03	1.627e-05	3.028e-08	*1*	0.00000	0.00003	0.00006
				2	0.00002	0.00004	0.00006
				3	0.00002	0.00004	0.00011

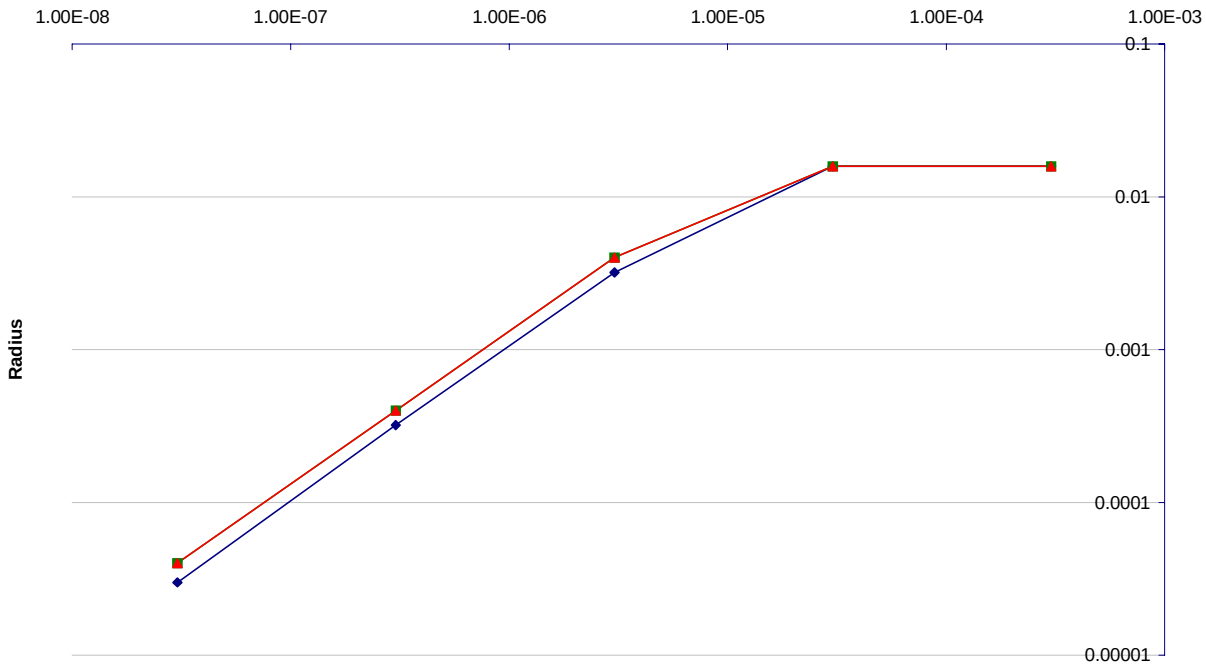

FIGURE 4.4.1 - Stabilizability Radius (5 radial, 10 angular segments)

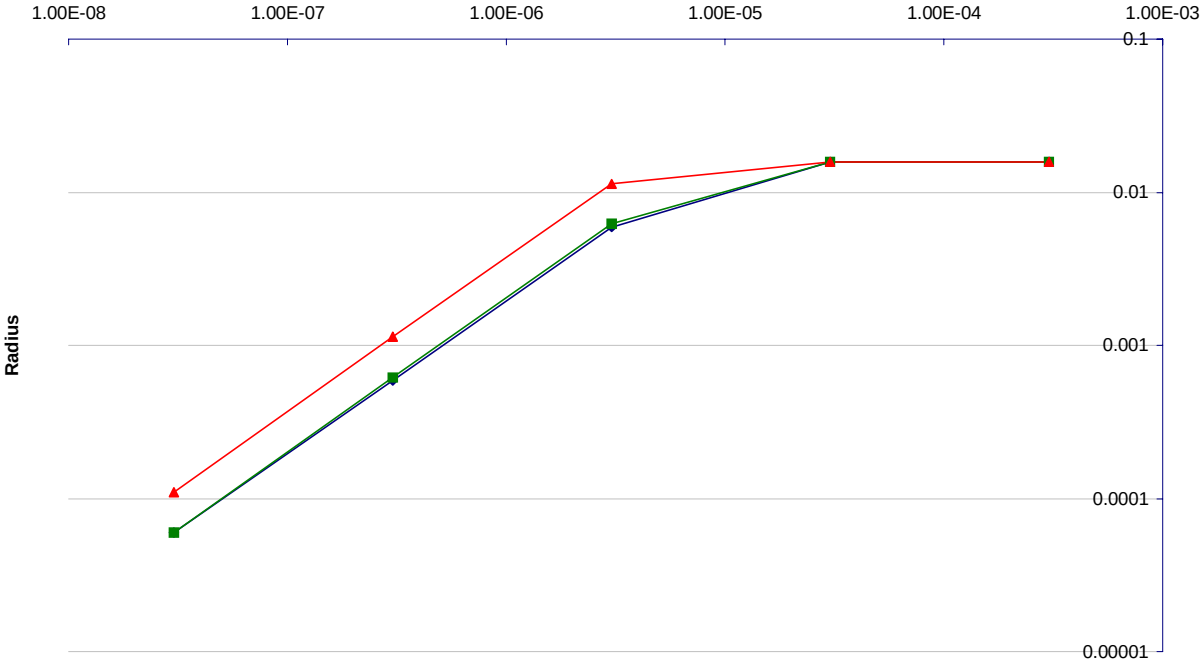

FIGURE 4.4.2 - Stability Margin (5 radial, 10 angular segments)

4.5 Conclusions

Calculating the controllability radii is demanding both in time and computing system capabilities. To determine the controllability radii with any accuracy requires an exhaustive search of the perturbations on the complex plane. One must find nearly all of the relative minimums to be certain of the results reliability.

We note that in most numerical runs, $\gamma_s = \sigma_{\min}[H(0)]$. However, there are no theoretical results that imply this result since $\mathbf{A} \neq \mathbf{A}^T$.

In general, the system properties behaved as expected relative to the control cases. Case 1 values were usually lower than Case 2, and Case 2 properties were usually lower than Case 3.

Smaller values for kinematic viscosity and larger values of the thermal expansion coefficient can reduce system stabilizability and stability. However, larger values of thermal diffusivity help achieve higher values for the stabilizability radius of the open loop system, [**A B**], and the stability margin for the closed loop system, [**A**-**BK**].

References

[1] Arnold III, W. F., and A. J. Laub*, Generalized Eigenproblem Algorithms and Software for Algebraic Riccati Equations*, Pro. IEEE, 12 (1984), 1746-1754.

[2] Belevitch, V., “Classical Network Theory,” Holden-Day, San Francisco, California, 1968, 413-414.

[3] Burns, J. A., and G. H. Peichl, *Open questions concerning approximation and control of infinite dimensional systems*, preprint.

[4] Burns, J. A., B. B. King, and D. Rubio*, Feedback Control of a Thermal Fluid Using State Estimation*, IJCFD, 11 (1998), 93-112.

[5] Creveling, H. F., J. F. De Paz, J. Y. Baladi, and R. J. Schoenhals, *Stability Characteristics of a Single-Phase Free Convection Loop*, J. Fluid. Mech., 67 (1975), 65-84.

[6] Demmell, J. W., *On condition numbers and the distance to the nearest illposed problem*, Numer. Math., 51 (1987), 251-289.

[7] Demmell, J. W., and B. Kagstrom, *Accurate solutions of illposed problems in control theory*, SIAM J. Matrix Anal. Appli., 9 (1988), 126-145.

[8] Eising, R., *The distance between a system and the set of uncontrollable systems*, Proc. MTNS-83, Beer Sheva, Lecture Notes in Control and Information Sciences, 58 (1984), 303-314, Springer, New York.

[9] Golub, G. H., and C. F. Van Loan, “Matrix Computations,” 3rd ed., Johns Hopkins University Press, Baltimore, Maryland, 1996.

[10] Hill, P., and C. Peterson, “Mechanics and Thermodynamics of Propulsion,” 2nd ed., Addison Wesley Publishing Company, Reading, Massachusetts, 1992.

[11] Kailath, T., “Linear Systems,” Prentice Hall, Englewood Cliffs, New Jersey, 1980.

[12] Kenney, C., and A. J. Laub, *Controllability and stability radii for companion form systems*, Math. Contr. Signals, Syst., 1 (1988), 239-256.

[13] Laub, A. J., *Computation of ‘balancing’ transformations*, Proc. JACC, paper FA8-E, 1980.

[14] Laub, A. J., *Numerical linear algebra aspects of control design computations*, IEEE Trans. Automat. Control, 30 (1985), 97-106.

[15] Oates, K. L., *A Study of Control System Radii for Approximations of Infinite Dimensional Systems*, Masters Thesis (1991), Virginia Polytechnic Institute and State University.

[16] Pazy, A., “Semigroups of Linear Operators and Applications to Partial Differential Equations,” New York, Springer, 1983.

[17] Rosenbrock, H. H., “State Space and Multivariable Theory,” John Wiley and Sons, New York, 1970.

[18] Rubio, D. *Distributed Parameter Control of Thermal Fluids*, Ph.D. Dissertation (1997), Virginia Polytechnic Institute and State University.

[19] Singer, J., Y. Wang and H. H. Bau, *Controlling a Chaotic System*, Phys. Rev. Lett., 66 (1991), 1123-1125.

[20] Wang, Y., J. Singer and H. Bau, *Controlling Chaos in a Thermal Convection Loop*, J. Fluid. Mech., 237 (1992), 479-498.

Julie Carlisle Albanus

A 1990 graduate of Virginia Polytechnic Institute and State University with a Bachelor’s of Science in Mathematics, Julie C. Albanus has returned to her alma mater to continue her studies as a part of the Interdisciplinary Applied Mathematics Program. Lieutenant Albanus currently serves in the United States Navy as an Engineering Duty Officer and is stationed in Arlington, Virginia.